A. JAMES CLARK
SCHOOL OF ENGINEERING

Future Trends of Nuclear and Raduion Applications in Nanotechnology

Mohamad Al-Sheikhly
Department of Material Science and Engineering
University of Maryland, USA

LAS/ANS
Rio de Janeiro, Brazil
June 21-25, 2010

Emerging Nanotechnologies in which Nuclear Applications and Radiation Play Key Roles:

- Nano-electronics
- Biotechnology
- Diagnostics
- Therapy

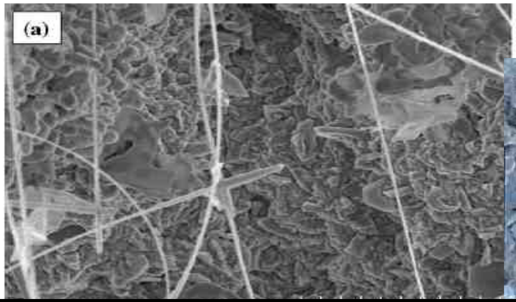

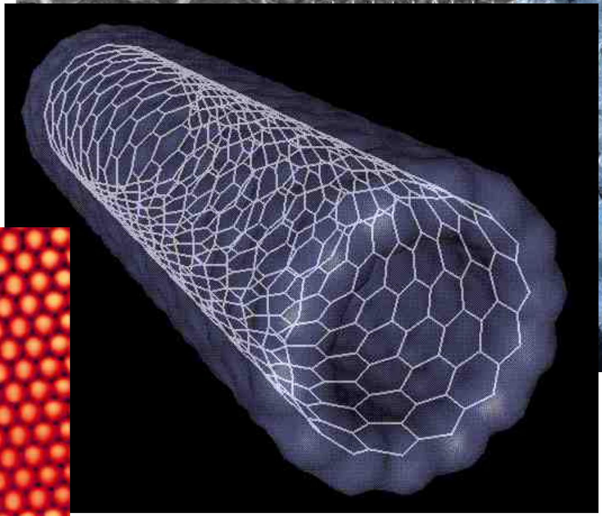

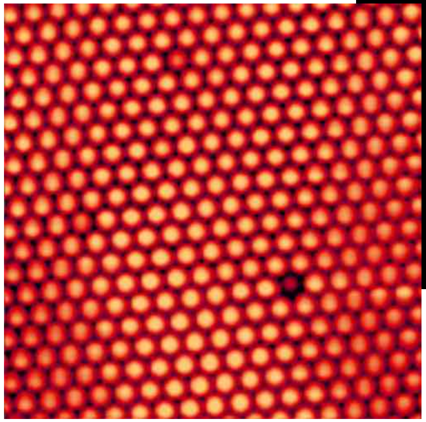

A. JAMES CLARK
SCHOOL OF ENGINEERING

Outline of Nanotechnology Utilizing the Following Types of Radiation:

- *Neutrons* for nanostructure characterization using small angle neutron scattering (SANS), positron generation, and nano-dosimetry modeling.
- *Heavy charged particles* for brachytherapy nano-dosimetry and electronics testing in high radiation environments.
- *Electron beam irradiation* for nanogel formation (drug delivery) and nanotube hardening.
- *Gamma-ray irradiation* for size control of nanoparticles.

Small Angle Neutron Scattering (SANS)

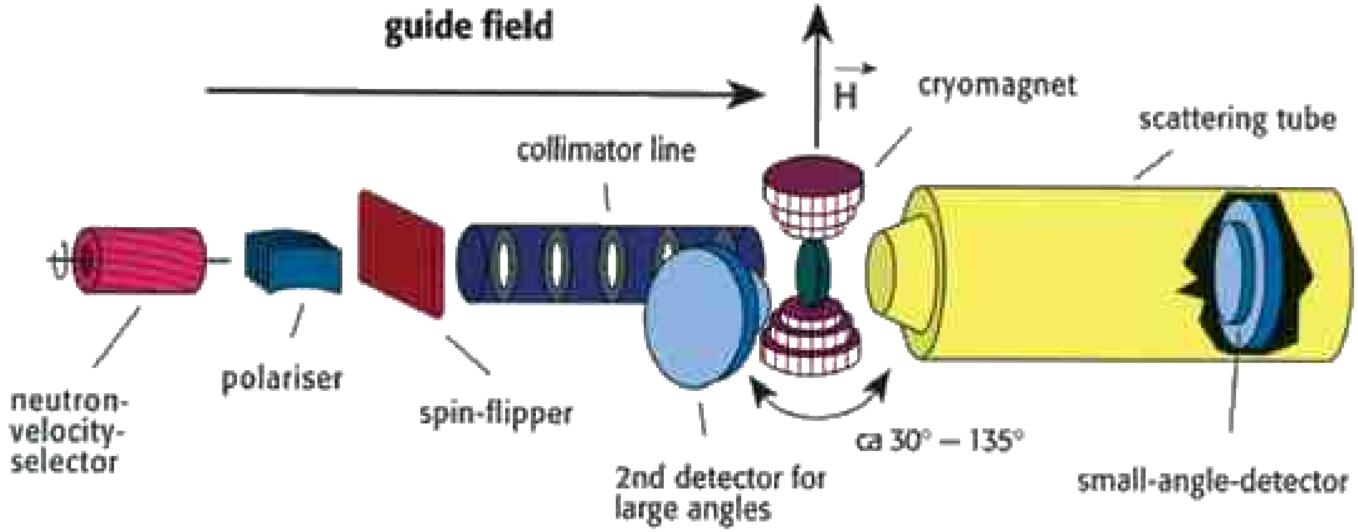

pathfinder.neutron-eu.net/idb/methods/sas

- SANS is a non-destructive method for determining the nanostructures of various samples through the analysis of scattering patterns caused by inhomogeneities within the sample.
- The study of soft matter and biological structures has been greatly impacted by “contrast variation”, a technique based on the ability to alter scattering length densities through the modification of isotopes within the sample.

SANS Determination of Unilamellar Vesicle Properties

- SANS investigation of unilamellar vesicles (nano-scale drug delivery) determines vesicle size and internal structure of lipid bilayer.
  - Thickness of bilayer
  - Thickness of hydrophobic and hydrophilic regions
  - Surface area of the membrane
  - Water molecules within the bilayer
- SANS also allows studies of dilute vesicular systems (1-2% w/w)

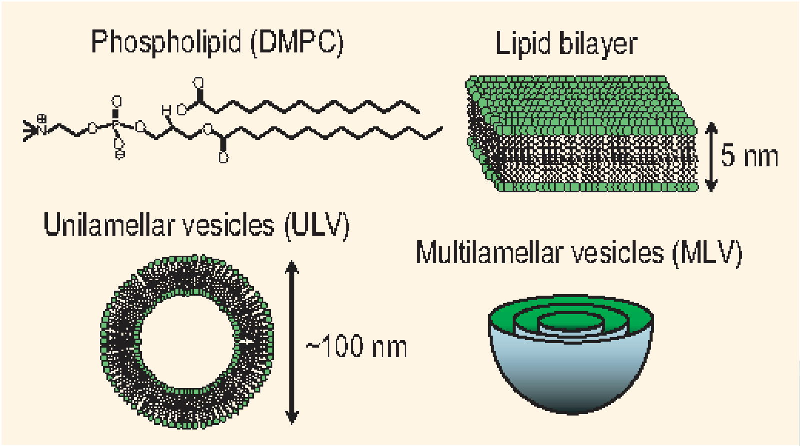

Fig. 1. Illustrations of a typical phospholipid (DMPC), a phospholipid bilayer, a unilamellar vesicle and a multilamellar vesicle.

www.ncnr.nist.gov/

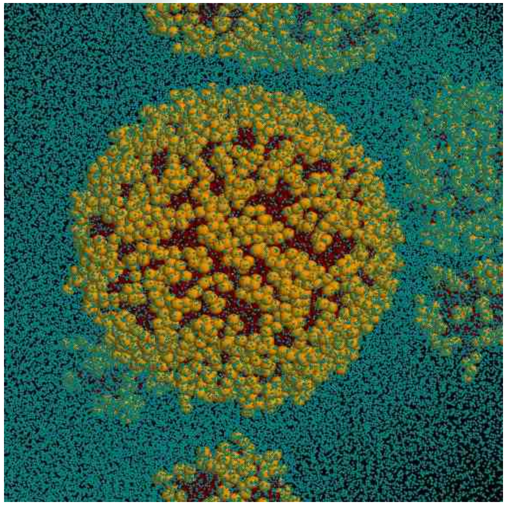

Zemlyanaya et al. *Crystallography Reports* 2006

md.chem.rug.nl/~marrink/science.html

Neutron Scattering Characterization of Nano-structures

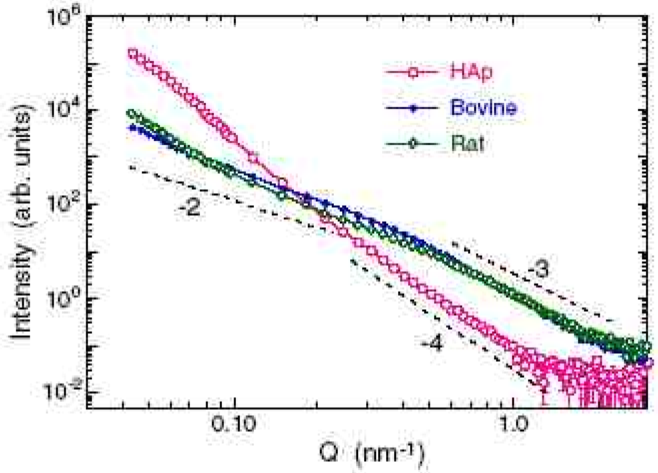

Figure 2. The small-angle neutron scattering profiles of an HAp powder, and the bovine and rat bone crystals at ambient temperature. The dashed lines are power-law behaviour denoted by the slopes for comparison with the different regions of the observed profiles.

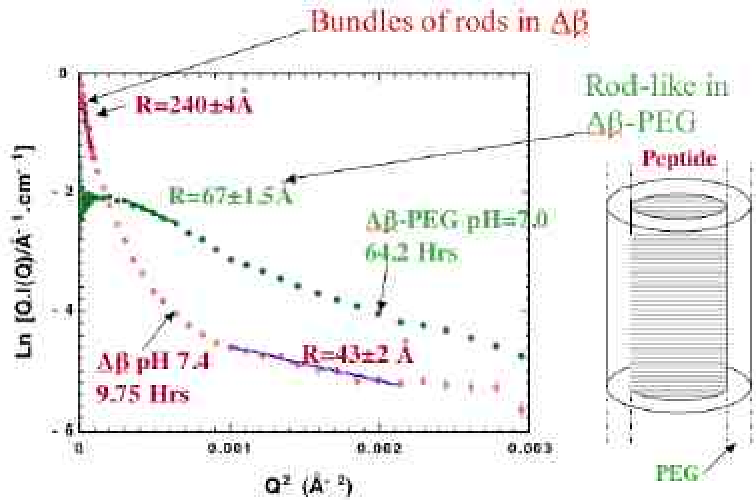

Figure 4. Modified Guinier plots of SANS data for $A\beta_{10-35}$ and $A\beta_{10-35}$-PEG solutions at pH ~7. $A\beta_{10-35}$ forms fibre bundles whereas the $A\beta_{10-35}$-PEG forms fibres of a single radius (mean radius 67 ± 1.5 Å) with a peptide core and a PEG shell (right).

SANS characterization of bone apatite nanostructure will influence the development of Hap-based biomaterials used to emulate bone materials.

SANS investigation of peptide self-assembly within biological systems reveals key information about how Alzheimer's disease is formed within the brain.

Loong et al. *Nanotechnology* 2004

A. JAMES CLARK
SCHOOL OF ENGINEERING

Neutron Scattering and Nanotechnology

Collaborations between the **NIST Center for Neutron Research** and the **Materials Science and Engineering Department at the University of Maryland**

Sampling of Techniques

- Neutron Diffraction
- Small Angle Neutron Scattering
- Triple Axis Neutron Spectroscopy
- Residual Stress Diffractometer
- Backscattering Spectrometer
- Spin Polarized Triple Axis
- Time of Flight Spectrometer
- Neutron Reflectivity
- Neutron Imaging
- Prompt Gamma Activation
- Neutron Spin Echo Spectrometer

Types of Problems

- Structure of active materials (piezoelectric, ferroelectric, shape-memory, magnetic, etc)
- Nanoporous materials, block copolymer structure, biopolymer folding, protein complexes
- Multilayer thin films for spintronics
- Polymer nanocomposites
- Spin correlations in superconductors
- Structure of PEM fuel cell membranes
- Surfactant and membrane characterization
- Carbon nanotube and C_{60} dispersions
- Nanodroplet nucleation and size evolution

Neutron Scattering ⟷ Nanotechnology

Ideally matched length scales

Some Examples

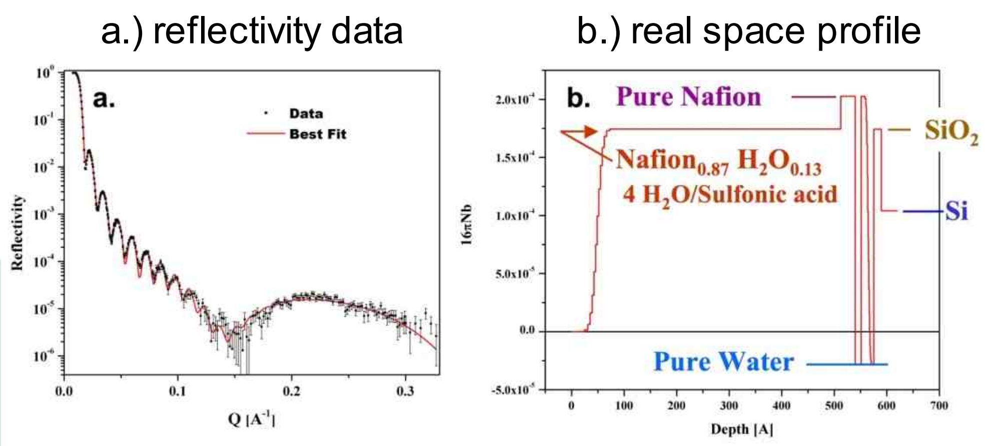

Neutron reflectivity data of water distribution within a model Nafion® PEM fuel cell membrane. Dura, J.

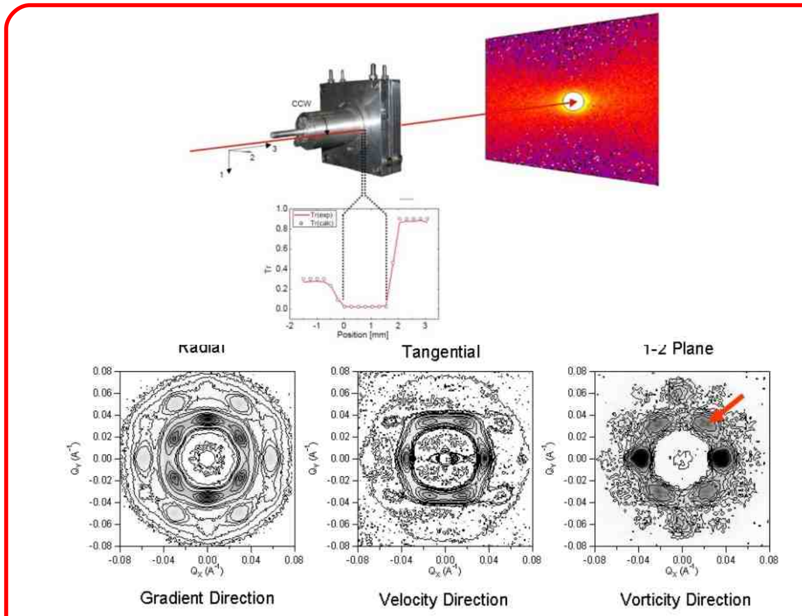

Schematic of *in-situ* shear cell for studying nanostructured fluids by small angle neutron scattering and data from FCC pluronic solution, D.C. Pozzo, L. M. Walker.

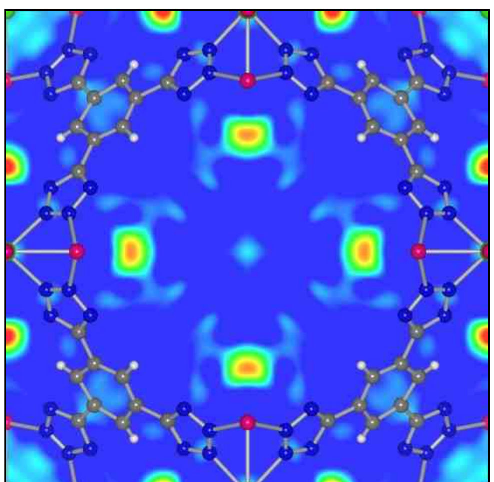

Hydrogen molecule adsorption sites (red-yellow regions) in Mn-BTT (Mn - 1,3,5 benzenetristetrazolate) determined by neutron diffraction. This material is a metal organic framework candidate material for hydrogen storage. M. Dinc; A. Dailly; Y. Liu; C.M. Brown; D.A. Neumann; J.R. Long

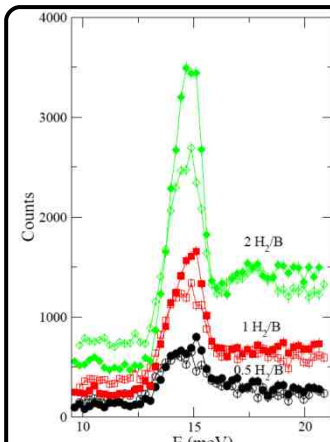

Neutron spectra of laser-produced single wall carbon nanotubes which are potential hydrogen storage materials. C.M. Brown, T. Yildirim, D.A. Neumann, M.J. Heben, T. Gennet, A.C. Dillon, J.L. Alleman, and J.E. Fischer

A. JAMES CLARK
SCHOOL OF ENGINEERING

North Carolina State University
PULSTAR Positron Beam
Nano-phase Investigation Using Anti-matter

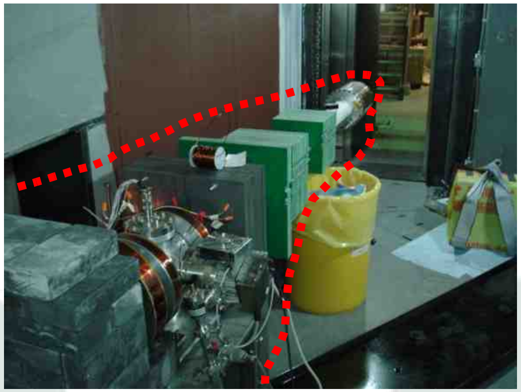

The positron beam-line (within the red border) prior to insertion into the PULSTAR reactor's beam port #6. The beam-line is ~15 feet long.

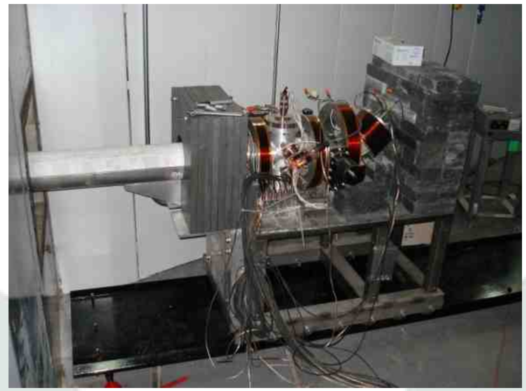

The positron beam-line partially inserted into the PULSTAR reactor's beam port #6.

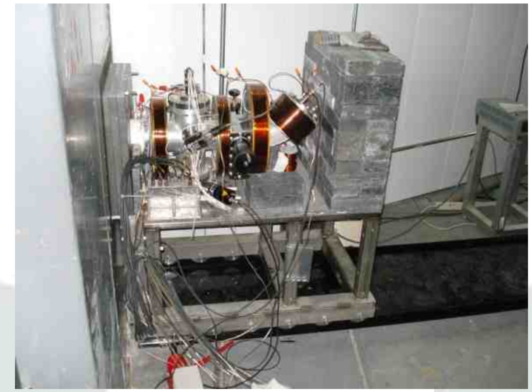

The positron beam-line fully inserted into the PULSTAR reactor's beam port #6.

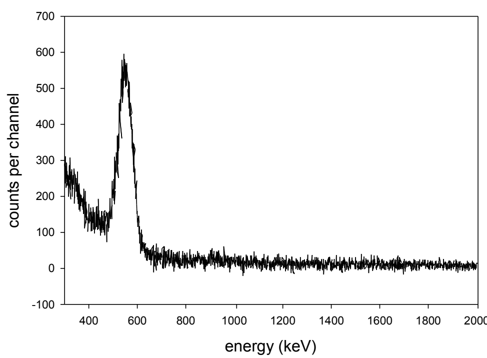

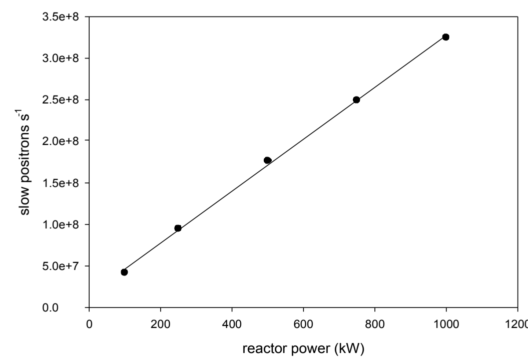

Recent results of positron generation by the PULSTAR reactor using the positron beam-line shown above. The results indicate a beam intensity exceeding **3×10^8 e+/s** at full reactor power (1-MW). On-going modification to the beam-line are expected to raise this number substantially. The figure on the left shows the signal of e^- - e^+ annihilation (i.e., 511 keV gamma-rays) in the detector.

For more information contact: **Ayman Hawari** ayman.hawari@ncsu.edu

A. JAMES CLARK
SCHOOL OF ENGINEERING

Characterization of Nano-structural Changes via Positron Annihilation Spectroscopy

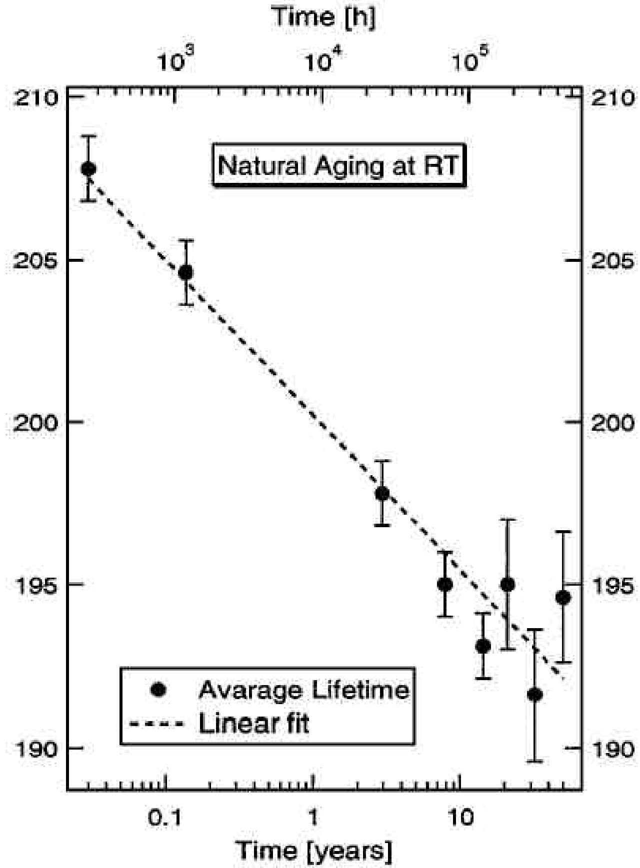

Figure 4 Change of the average positron lifetime with the duration of natural ageing of the 2024 T3 alloy.

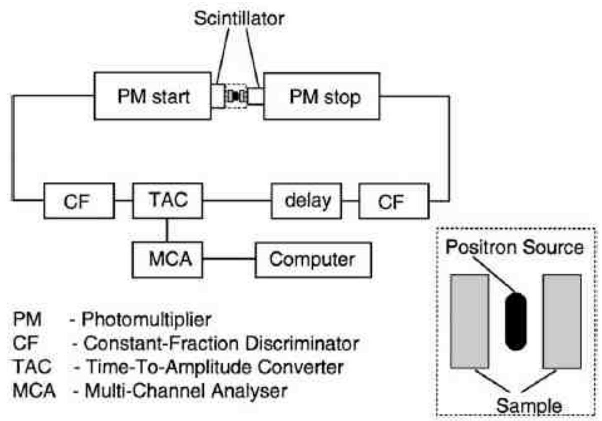

Figure 1 Principle of lifetime measurement: the source-sample arrangement is magnified.

- Positron lifetimes and intensities change during natural and artificial aging.
- Changes can be detected in nano-structure which are not measurable in certain material properties (i.e. hardness).

Staab et al. *Journal of Materials Science* 2000

Nano-dosimetry Cell Survival Model in Mixed LET Field

- New nano-dosimetry model is based on LQ formula but employs physical and biological quantities and is ideal for predicting cell survival in mixed LET radiation fields.
- Physical quantities relate to energy deposition on the DNA and chromatin scales (5 nm and 25 nm).
- Biological quantities relate to probabilities of lesion production and interaction, as well as lesion repair rate.

$$-\ln(S_{n\gamma}) = \alpha_n D_n + \beta_n D_n^2 + \alpha_\gamma D_\gamma + \beta_\gamma D_\gamma^2 + \beta_{n\gamma} D_n D\gamma$$

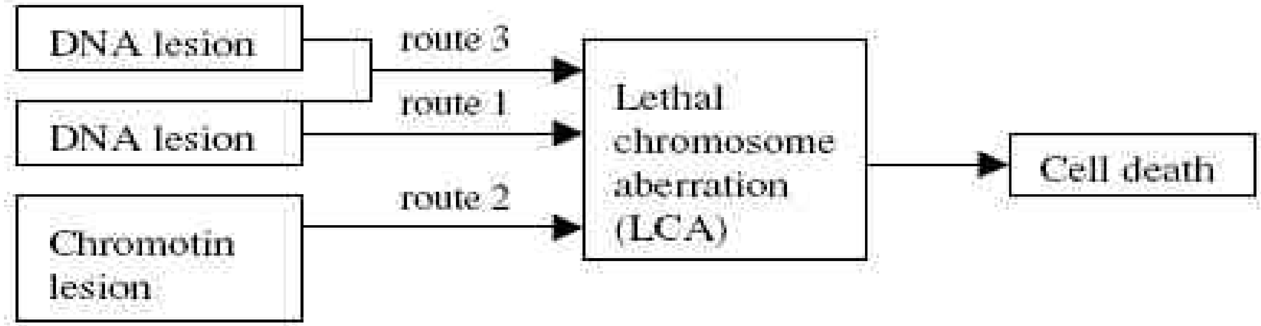

Figure 1. The schematic diagram of the new cell survival model showing the two lesion types (DNA and chromatin) and how they are related to the three biological pathways leading to cell death.

Wang et al. *Phys. Med. Biol.* 2006

Nano-dosimetry Cell Survival Model in Mixed LET Field

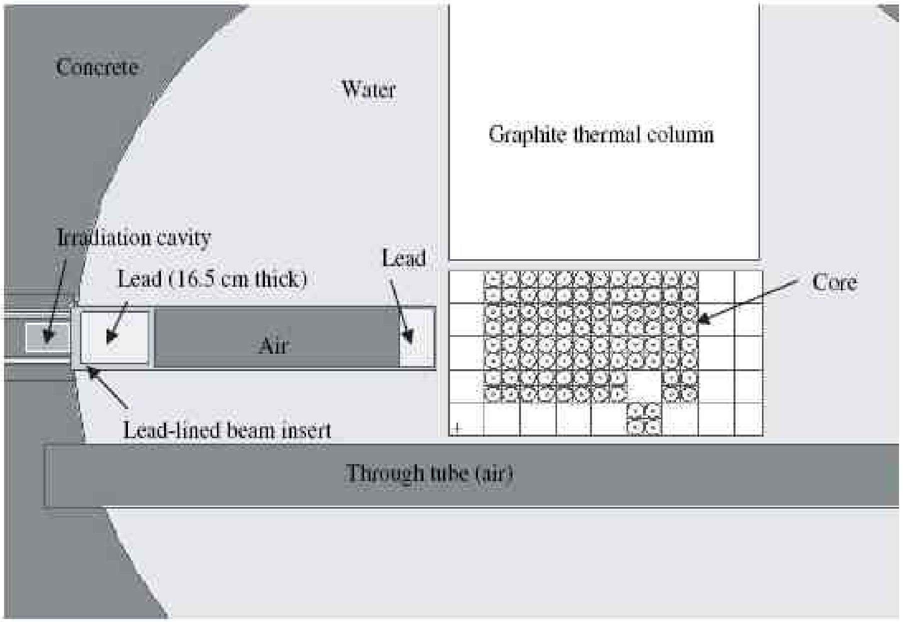

Figure 1. The two-dimensional MCNP model of the MUTR core and the irradiation beam port.

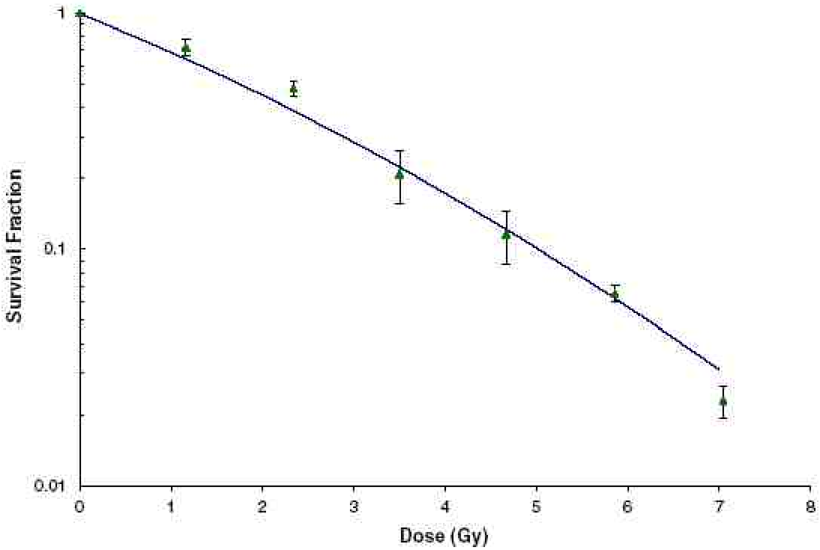

Figure 4. The experimental survival data (▲) and the survival curve predicted by the new model (i.e. equation (3)) for V-79 cells irradiated with the mixed neutron and gamma-ray irradiation at the MUTR.

- Experimental validation was performed at MUTR facility with a mixed LET field of neutrons and gamma-rays.
- Provides validation of new nano-dosimetry model to be used to mixed LET radiotherapies (i.e. ^{252}Cf brachytherapy).

Wang et al. *Phys. Med. Biol.* 2006

Boron Neutron Capture Therapy (BNCT)

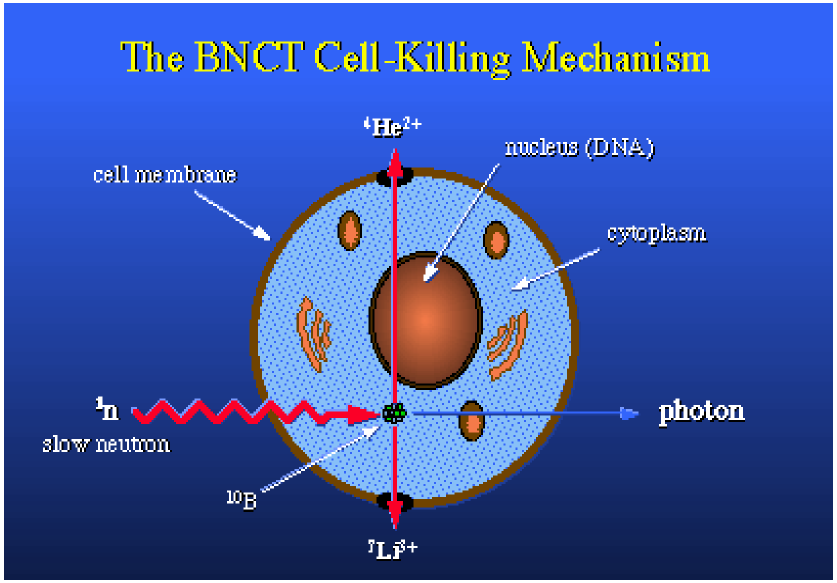

- Low-energy neutrons interact with ^{10}B isotope to produce high-energy and short-range alpha particles and ^7Li.
- High LET alpha particles have a very short path length (<10μm).
  - Neighboring cells will be unaffected.
- Particles release 200keV/μm within the cell.
  - Only a few particles are required to kill a cell.
- Cancer tumor in the prostate can be targeted with a direct neutron beam due to its favorable location (away from vital organs).

A. JAMES CLARK
SCHOOL OF ENGINEERING

Heavy Ion Irradiation of Nanowires and Nanocircuits

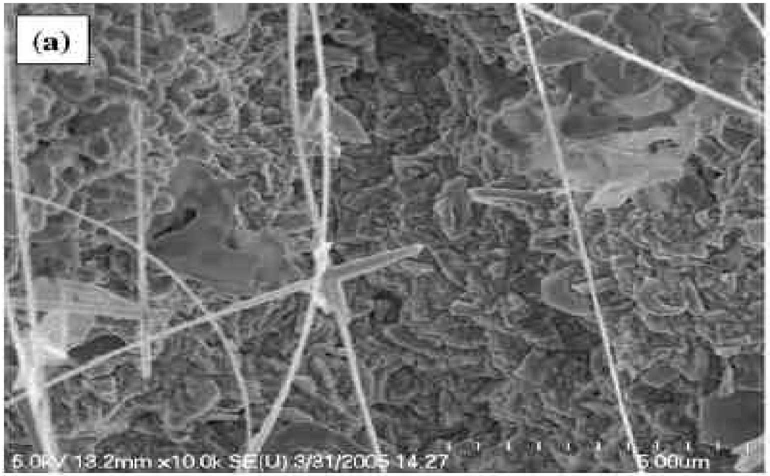

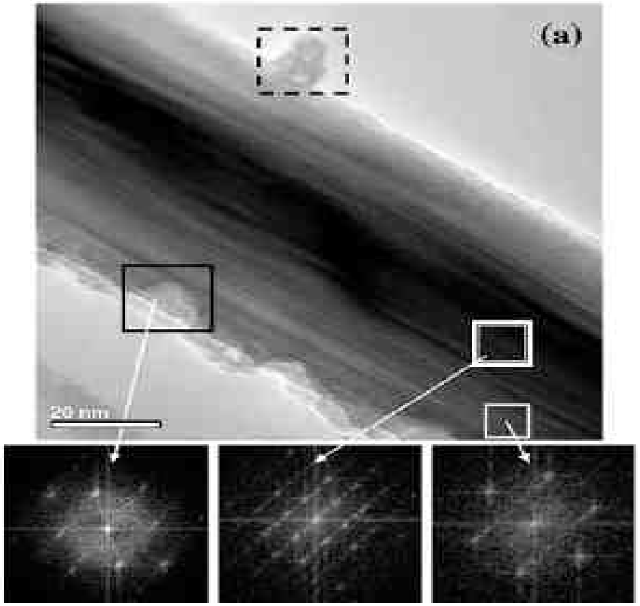

- GaN nanowire-based circuit is shown to exhibit real-time and post-irradiation operability upon exposure to ^{78}Kr heavy ions, demonstrating that this technology may be valuable in certain radiation environments.
- National Superconducting Cyclotron Lab at Michigan State University provides beam energies that closely match those found in space radiation environments.

Ayres et al. *Diamond and Related Materials* 2006

Nuclear Graphite Damage, Healing and Lifetime (Generation IV)

While the general effects of neutron irradiation on graphite are reasonably well understood, little data for irradiation behavior of graphite at temperatures above 1000 ^{o}C exist. It is also essential to gain a better understanding of the relationship between the rate of graphite degradation, the concentration of naturally occurring impurities in the graphite and impurities in the helium coolant.

Graphite

Understanding of the effects of neutron irradiation not only on the mechanical properties but also on the chemical properties of graphite. Clearly, there are many individual factors, such as neutron damage, graphite impurities, and diffusion of fission products that lead to the damage of graphite operating under reactor core conditions. In this proposal, we will estimate the result of all of these factors working together under the extreme conditions found in Generation IV – very high temperature reactors.

Graphite

While the general effects of neutron irradiation on graphite are reasonably well understood, little data for irradiation behavior of graphite at temperatures above 1000 °C exist. It is also essential to gain a better understanding of the relationship between the rate of graphite degradation, the concentration of naturally occurring impurities in the graphite and impurities in the helium coolant.

Graphite Oxidation by CO_2

Helium is the primary HTGR coolant and contains small amounts of impurities such as CO_2, H_2, H_2O, CH_4, CO, O_2

These impurities corrode graphite by oxidation.

The following CO_2 oxidation mechanisms are responsible for this corrosion:

$$C + CO_2 = 2CO$$

Other Oxidation Mechanisms

Oxidation by water:

$C + H_2O = CO + H_2$

$C + 2\ H_2O = CO_2 + 2H_2$

$C + 2H_2 = CH_4$




Oxidation by Oxygen:

$\frac{1}{2}\ O_2 + C = CO$

$O_2 + C = CO_2$

Proton Irradiation of Carbon Nanotubes (CNTs)

- Field effect transistors are fabricated from single-walled carbon nanotubes (SWNT) and based on their unique electric properties.
- High tolerance to 10-35 MeV protons with a fluence of $4x10^{10}$-$4x10^{12}$ cm^{-2} (comparable to aerospace environment) shows high radiation hardness of these devices.
- Electrical measurement and Raman spectra show no significant change in electronic properties following proton irradiation.

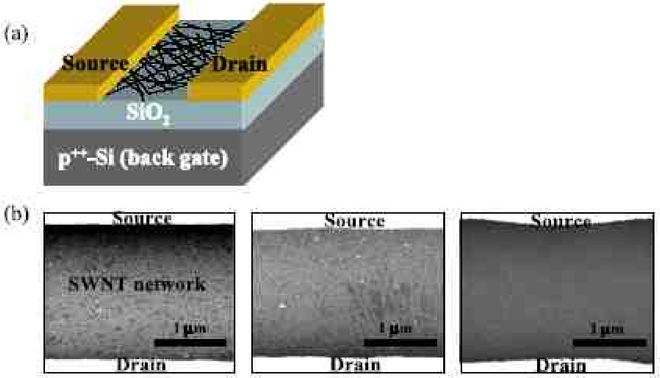

Figure 1. (a) Schematic drawing of single-walled carbon nanotube network field effect transistor (SWNT network FET). (b) SEM images of SWNT network FETs showing different densities of SWNTs connected between the source and drain electrodes.

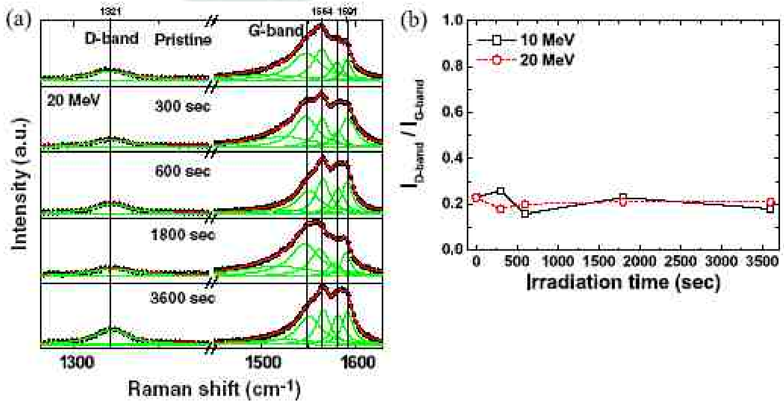

Figure 5. (a) Raman spectra at an excitation wavelength of 633 nm for the SWNT network FETs before (pristine) and after proton irradiation of 20 MeV for 300, 600, 1800, and 3600 s corresponding to the fluence of 1.2×10^{11}, 2.4×10^{11}, 6.9×10^{11}, and 1.4×10^{12} cm^{-2}, respectively. (b) The intensity ratio of D-band to G-band at different radiation time periods for 10 and 20 MeV proton beams.

Hong et al. *Nanotechnology* 2006

Global Applications of Ionizing Radiation

- Polymer crosslinking
- Graft polymerization
- Enzyme immobilization
- Controlled drug release
- Hydrogels and gel-filled membranes
- Used to create non-thromogenic surfaces
- Textile modifications for hydrophilicity, ion-exchange
- Membrane technology for chromatography
- Electron beam lithography
- Waste water treatment, ion-exchange, salt rejection
- Fuel Cell


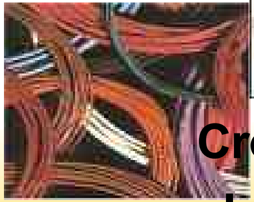


Crosslinking of electrical cable surfac

UHMWPE
Hip joint cup

Contact lens

Wound dressing

Sterilization process

Types of Radiation

- Alpha
  - He^{2+}
  - Very shallow penetration depths
- Beta
  - Electrons
  - Penetration depends on energy
- Photons
  - Gamma
  - X-ray
  - UV light

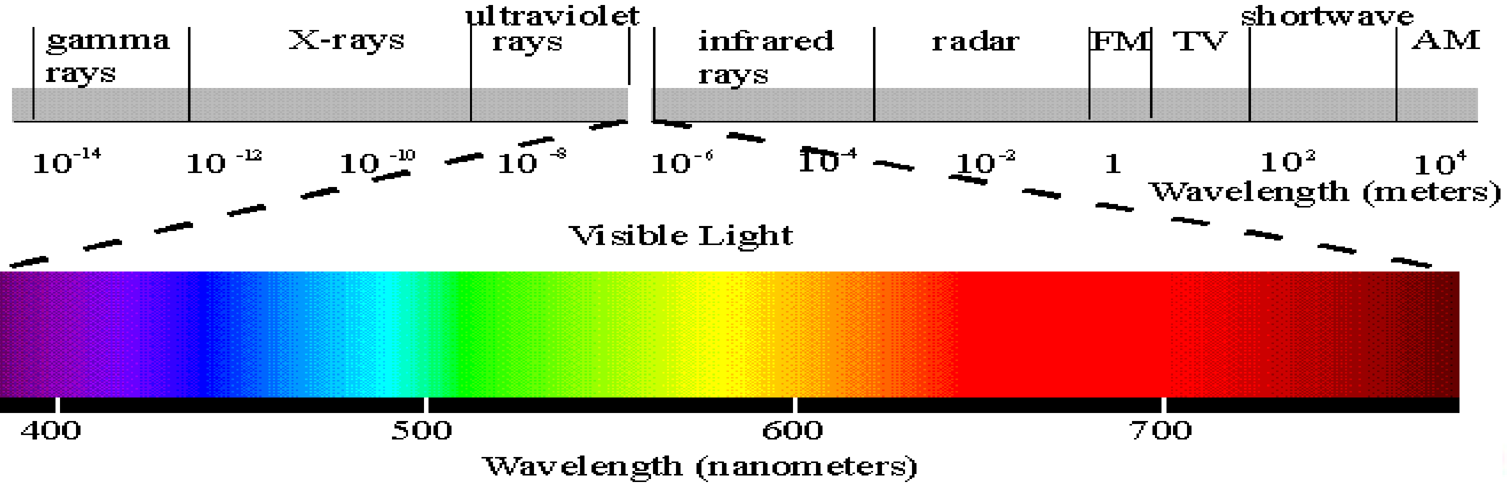

Electron Accelerator Schematic

A. JAMES CLARK
SCHOOL OF ENGINEERING

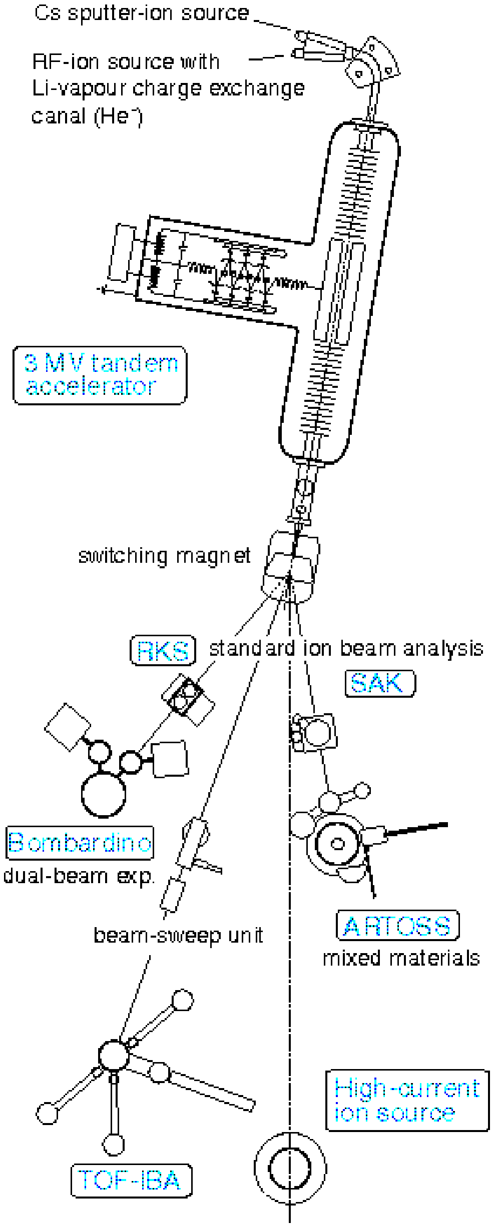

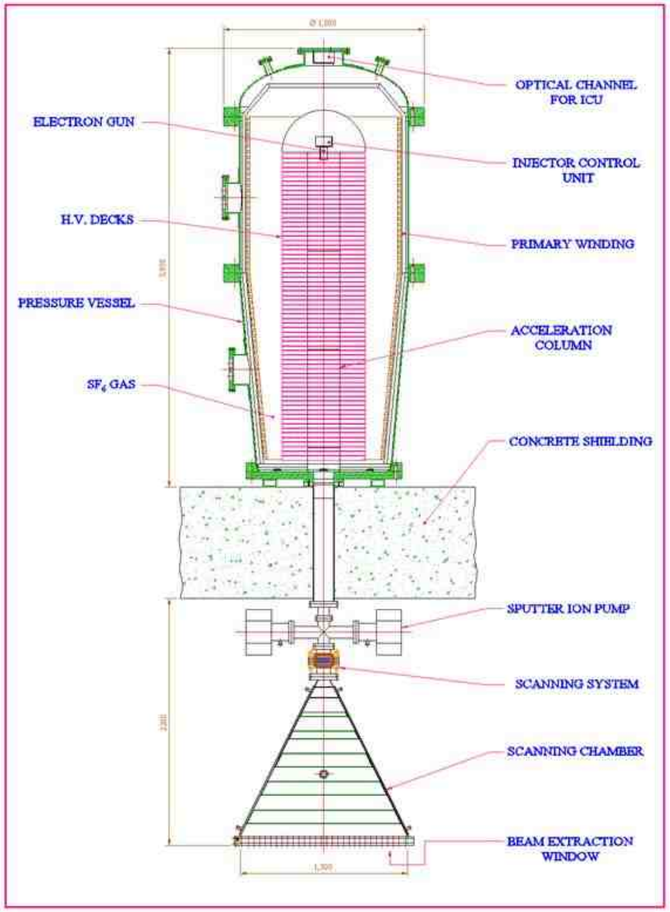

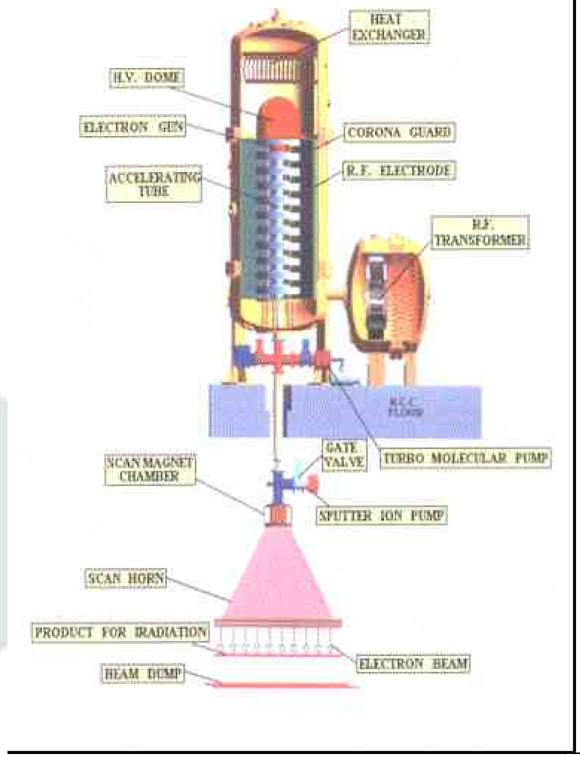

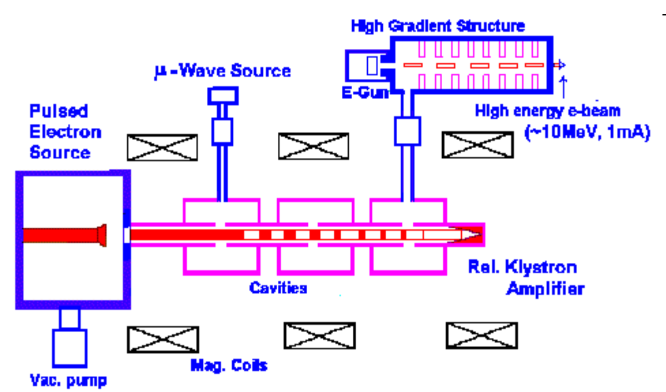

Interaction of Ionizing Radiation with Matter

10^{-18} 10^{-15} 10^{-12} 10^{-9} 10^{-6} 10^{-3} 1 sec

Energy deposition

- formation of ionized and excited molecules localized along tracks
- Ions and excited molecules react/dissociate forming free radicals. Electrons solvated in polar media

Chemical Processes

- Radicals and solvated electrons diffuse from track zones, react with other molecules.
- Chemical changes to substrate occur.

- Direct Effect
  - M $\rightsquigarrow$ M^+, e^-, M^* (Ionization, excitation)
- Indirect Effect
  - Secondary reactions of solute with primary species formed by solvent

Polymer Nano-hydrogels

A. JAMES CLARK
SCHOOL OF ENGINEERING

Objective

Synthesize bio-compatible polymer nano-hydrogels for biomedical applications (e.g., drug delivery systems) by using simple & efficient ionizing radiation processes.

Polymer Nano-hydrogel

3D polymer network & filling liquid (water) with diameter size range of 1 – 10^2 nm

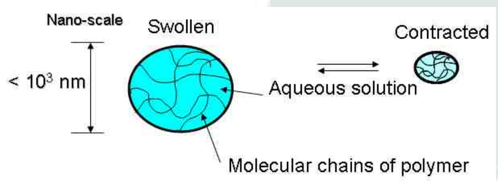

Hydrogel in Nano-Technologies

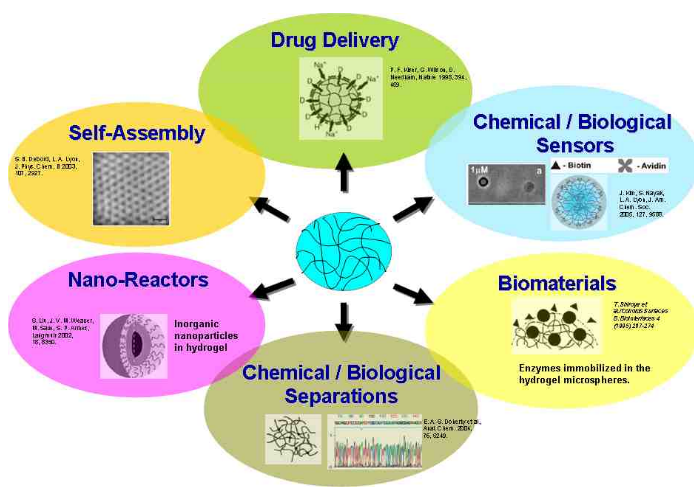

Size Matters!

Size (within nanoscale) strongly affects circulation time in blood and bioavailability of the particles within the body by evading RES (reticulo endothelial system).

Particle diameter (nm)	Effects
5-10	Removal through extravasation & renal clearance
10 - 70	Penetrate very small capillaries within body tissues → most effective distribution in certain tissue
70 - 200	Longest circulation times
> 200	Filtration by spleen → removal by phagocyte system → decreased circulation times

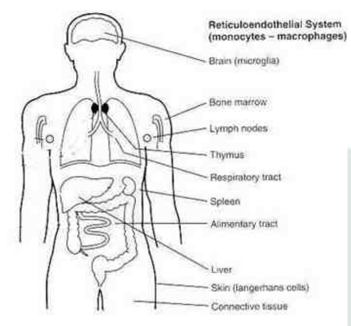

Target-specified Drug Delivery

Permeation and retention of polymer nano-hydrogel drug conjugates via leaky tumor vasculatures.

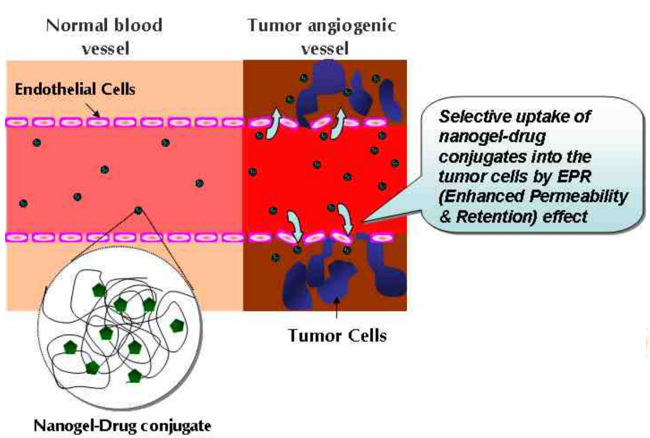

A. JAMES CLARK
SCHOOL OF ENGINEERING

Synthesis of Nano-hydrogel

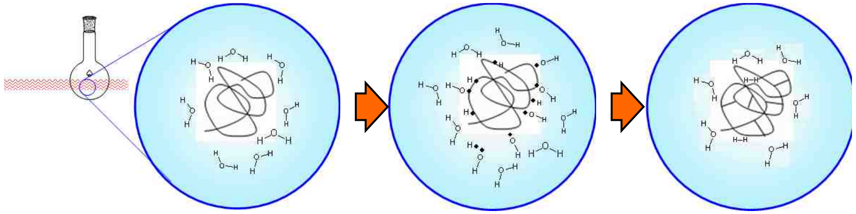

(1) Irradiation of dilute hydrophilic polymer aqueous solution (e.g., poly(vinyl pyrrolidone), PVP).
- •OH from the water radiolysis abstracts H from polymeric chain yielding C-radicals.
- C-radicals recombine producing cross-links

Inter- vs. Intra-crosslinking

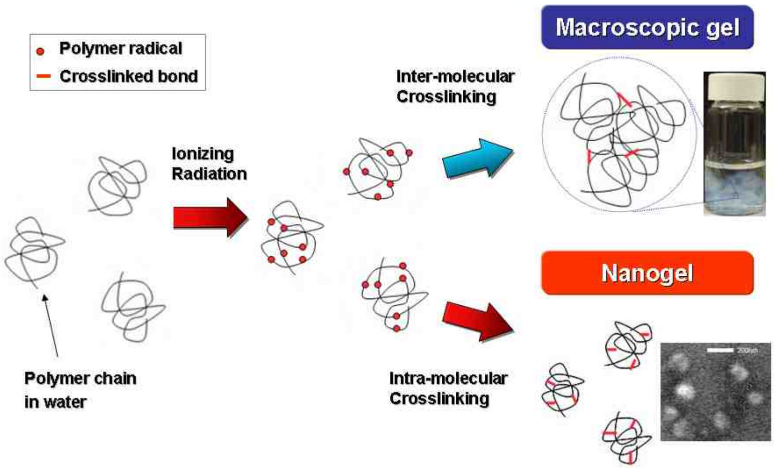

Parameter Effects on Nano-hydrogel Synthesis

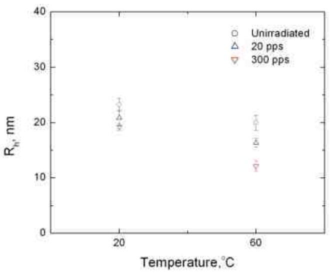

Higher Temperature (T)
Higher Pulse Repetition (PPS)
Higher Dose

enhance intramolecular crosslinking

Smaller nanogels (R_h)

Surface Morphology of Nano-hydrogel (AFM)

Unirradiated PVP (linear chain) shows flat surface morphology.

PVP nanogel shows spherical contour of surface.

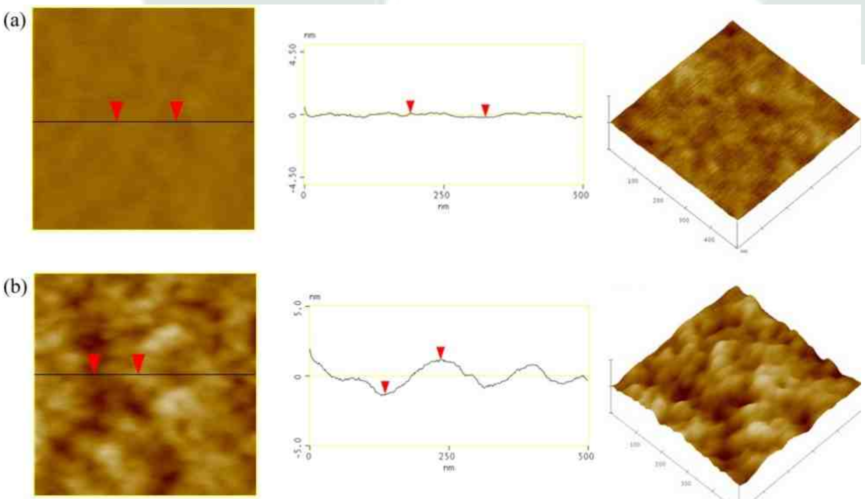

Pulse Radiolysis for Nanogel Synthesis

A. JAMES CLARK
SCHOOL OF ENGINEERING

- **Fast chemical reaction kinetics (rate constant, k) and radiation yield (G-value) can be studied in μ to nano second range.**

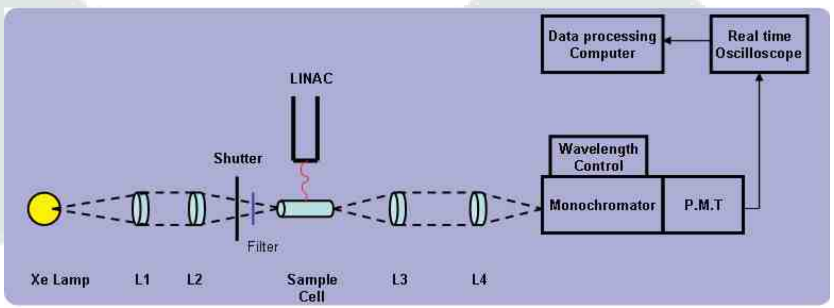

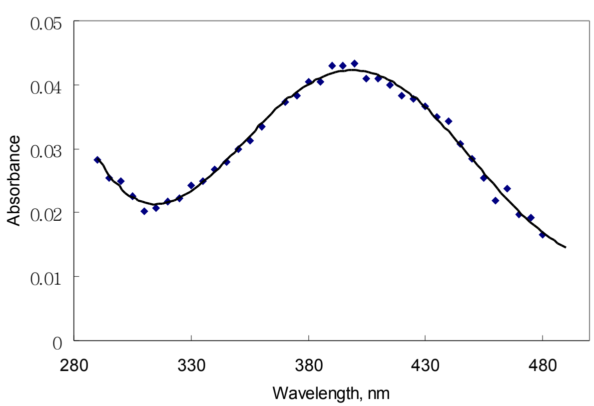

Absorption spectra of transient species form during pulse radiolysis of 0.009 M PVP solutions at RT

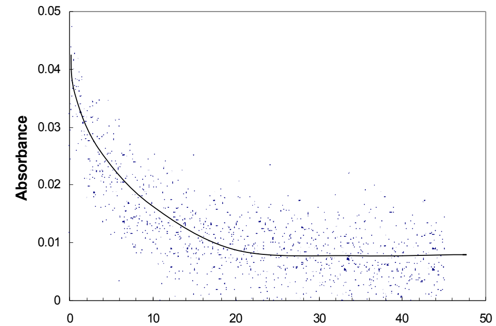

Decay profile of transient species at 390 nm

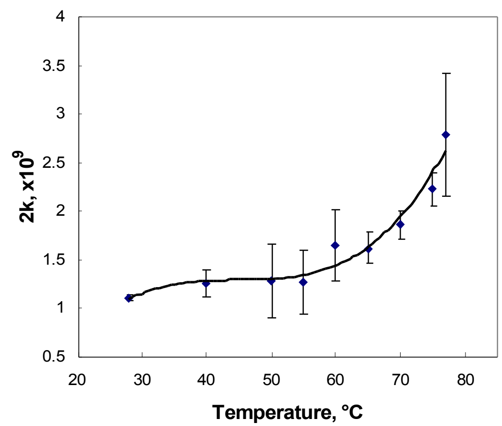

Change of second order reaction (bimolecular decay) rate constant as a function of temperature (a),

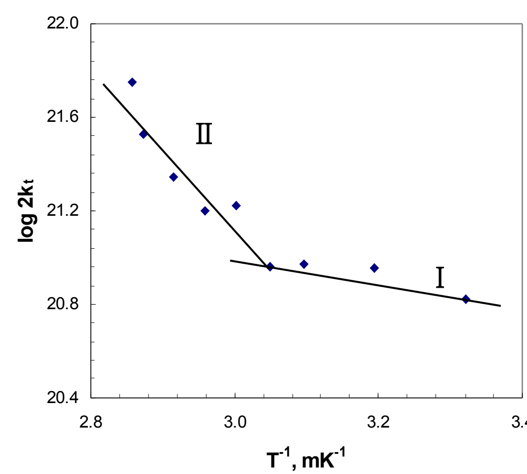

Arrhenius plot of PVP radical decay rate constant from which activation energies E_a = 1.0 kcal mol^{-1} (I) and 6.8 kcal mol^{-1} (II) were derived for two different temperature regions

A. JAMES CLARK
SCHOOL OF ENGINEERING

Structure Transformation of Nanotubes by E-beam Irradiation

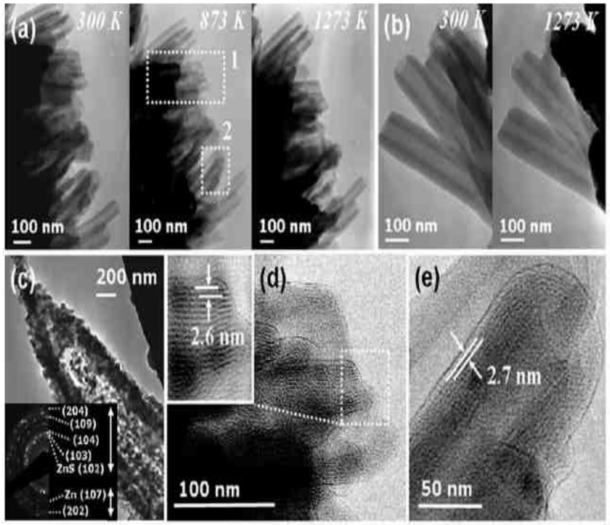

Fig. 3 *In-situ* TEM investigations of the thermal behavior of nanotubes. (a) TEM images of progressive heating from 300 K to 1273 K with nanotubes under nearly continuous electron irradiation. (b) TEM images taken at 300 K and 1273 K with the nanotubes under shorter electron-irradiation treatment time (5 min). (c) TEM micrograph of nanotubes without electron irradiation. Inset shows diffraction pattern indicating crystalline ZnS and Zn particles. (d,e) Enlarged TEM images from areas 1 and 2 of (a) taken at 873 K. Inset of (d) shows the fast-Fourier transform (FFT) image of the region indicated by the white-dotted square.

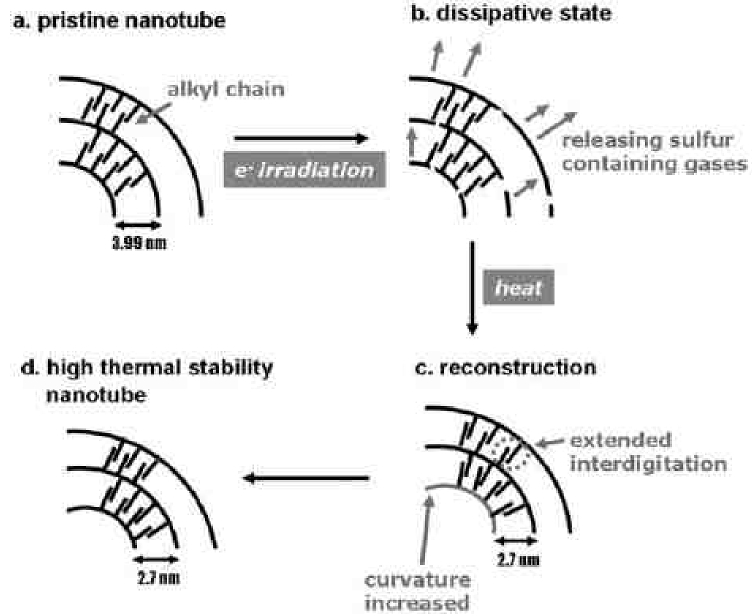

Scheme 1 Schematic illustration of high thermal stability nanotube formation mechanism.

- *In-situ* TEM has been used to show very high thermal-resistance of self-assembled supramolecular nanotubes.
- Breaking of chemical bonds and subsequent self-organization are considered important for the reconstruction of multi-shell structural transformation.

Huang et al. *Journal of Materials Chemistry* 2007

A. JAMES CLARK
SCHOOL OF ENGINEERING

Electron Induced Defects in Carbon Nanotubes

- Carbon nanotubes are very promising structures for molecular electronics.
- Small defects in the structure caused by electron irradiation can lead to drastically different electronic properties within the nanosystem.
- Understanding the mechanisms of carbon atom displacement and repair allow for tailoring of specific properties.

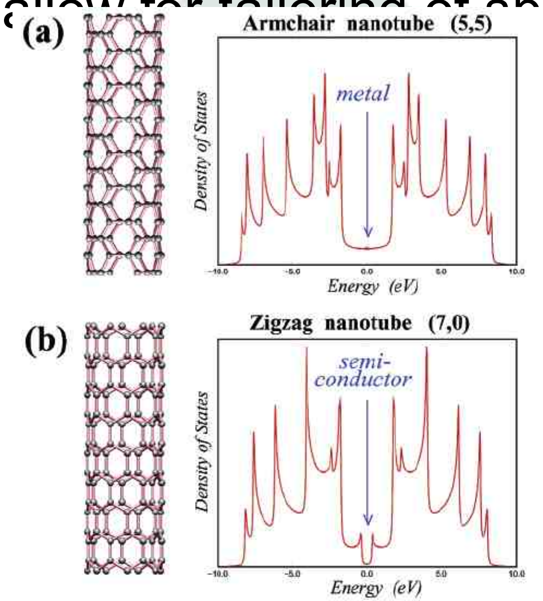

FIGURE 2. Electronic properties of two different carbon nanotubes. (a) The *armchair* (5,5) nanotube exhibits a metallic behavior (finite value of charge carriers in the DOS at the Fermi energy, located at zero). (b) The *zigzag* (7,0) nanotube is a small gap semiconductor (no charge carriers in the DOS at the Fermi energy). Sharp spikes in the DOS are van Hove singularities (a,b).

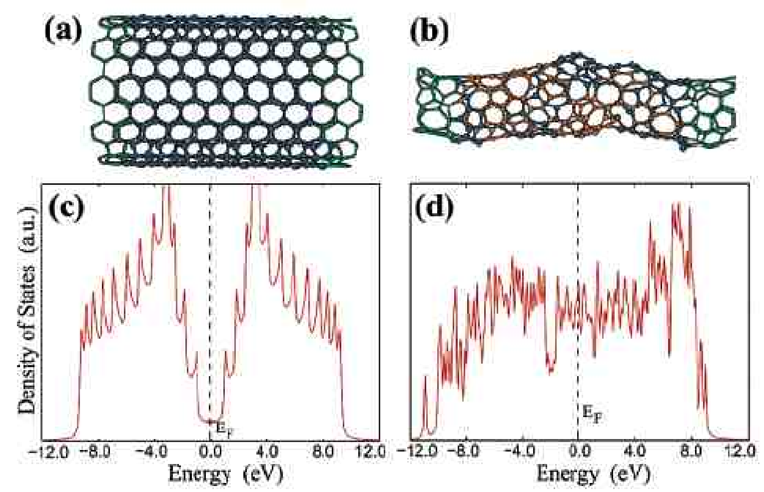

FIGURE 5. Surface reconstution of (a) a (10,10) single-wall carbon nanotube (ϕ = 1.36 nm) after a random extraction of 200 carbon atoms along the entire tube surface. Although the reconstructed surface is higly defective (b), the carbon system is still a rough cylinder, the diameter value of which is ~0.7 nm, containing 15 5/7 pair defects (in light brown). The corresponding electronic DOS are also illustrated in (c) and (d), respectively.

Charlier *Acc. Chem. Res.* 2002

Ionomer Templates for Nanocomposites

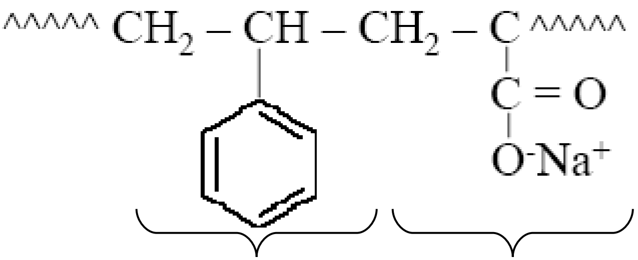

styrene

methacrylic acid neutralized with sodium

IONOMER: random copolymer containing small fraction (<15 mol%) of ionic segments

Poly(styrene-co-methacrylic acid):

- **$MAANa^{+}$ groups cluster together to form aggregates**
- **ionic aggregates ($MAANa^{+}$) separated from one another by the less polar segments (styrene)**

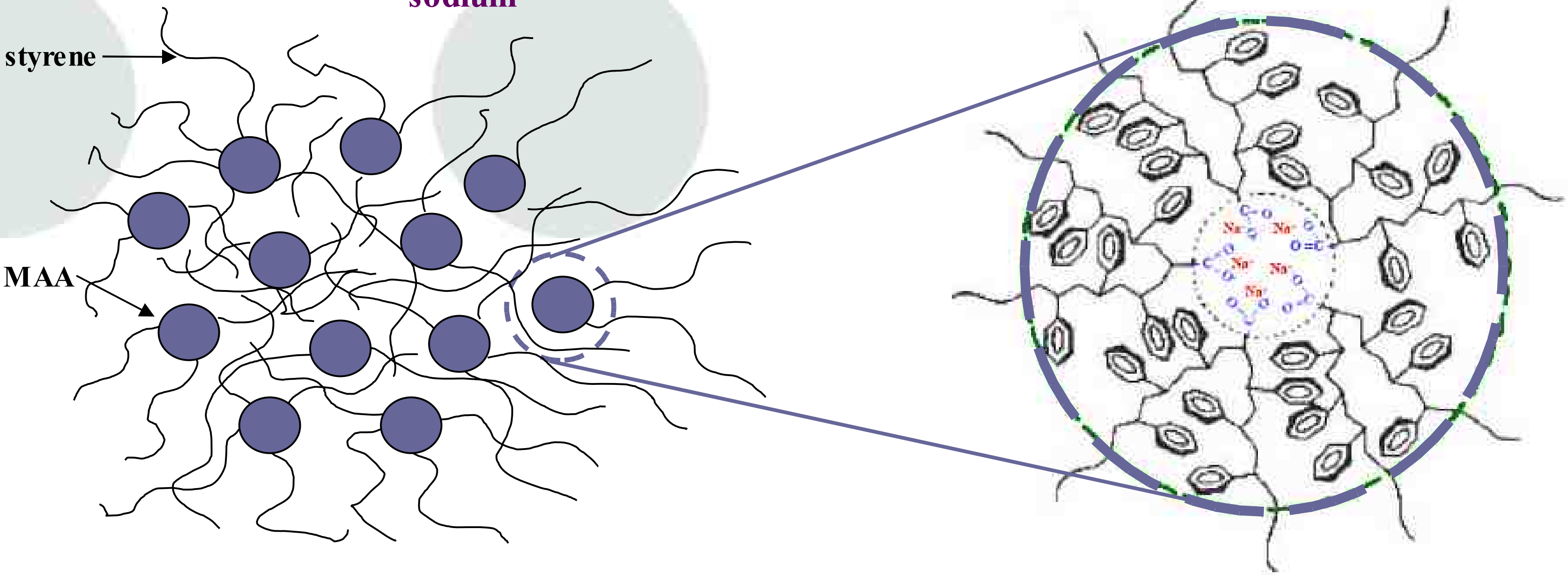

A. JAMES CLARK
SCHOOL OF ENGINEERING

Experimental Procedure

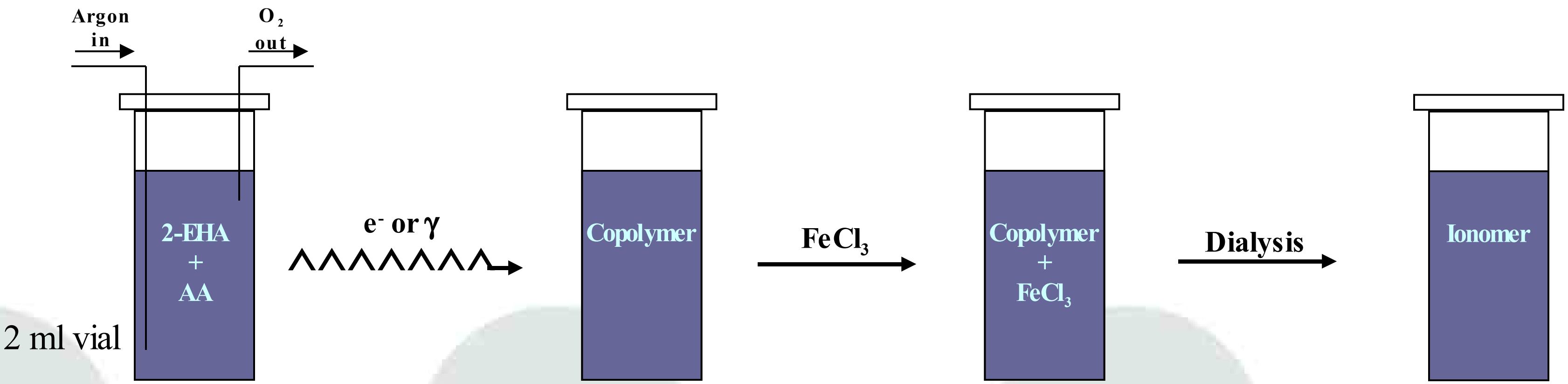

Purify 2-EHA/AA monomer mixture by bubbling with argon

Irradiate to produce 2-EHA/AA copolymer

Mix with metal salt

Remove unassociated ions to produce 2-EHA/AA/Fe^{3+} ionomer

$CH_2=CH-C(=O)-OR$ + $CH_2=CH-C(=O)-OH$

R = - $CH_2CH(CH_2CH_3)CH_2CH_2CH_2CH_3$

90 wt% EHA + 10 wt% AA
= 3.5 mol EHA : 1 mol AA

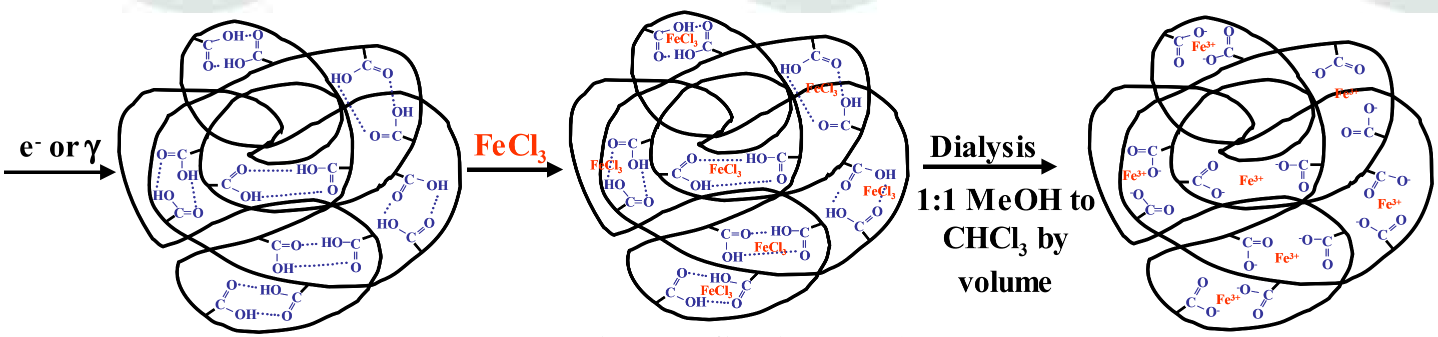

1 mol $FeCl_3$: 3 mole AA

A. JAMES CLARK
SCHOOL OF ENGINEERING

FTIR: Quantitative Analysis Method

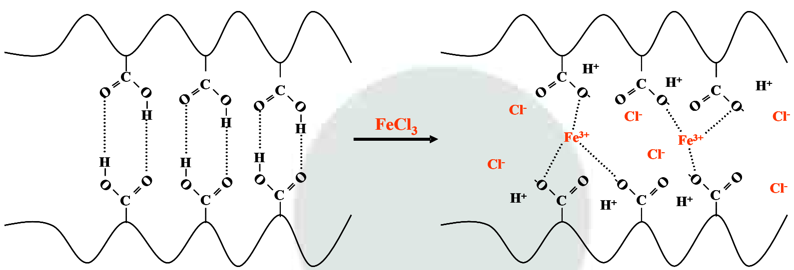

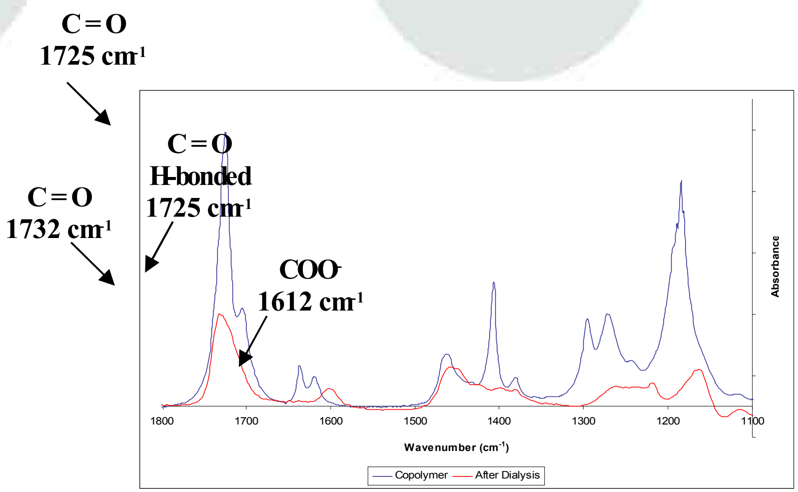

- Purpose: study hydrogen bonding, interactions between copolymer and metal via acrylic acid repeat units

Nanometer Gelatin Particles via Gamma-ray Irradiation

- Gelatin nanogels can be prepared with gamma-ray irradiation, without the use of chemical reagents.
- MW of nanoparticles increases while hydrodynamic radius decreases.
- Size is variable using control parameters.
- This technique has great promise in the field of BioMEMs.

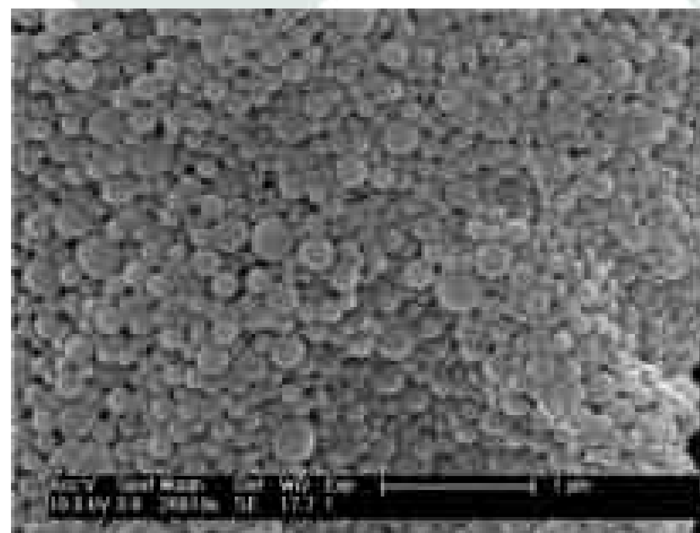

Furusawa et al. *Colloid Poly. Sci.* 2004

A. JAMES CLARK
SCHOOL OF ENGINEERING

Final Remarks

- At present, there are numerous emerging nanotechnologies that utilize neutrons, heavy charged particles, light charged particles, and electromagnetic radiation including but not limited to:
  - Nano-electronics
  - Biotechnology
  - Diagnostics
  - Therapy

FTIR: Ionomer Synthesis

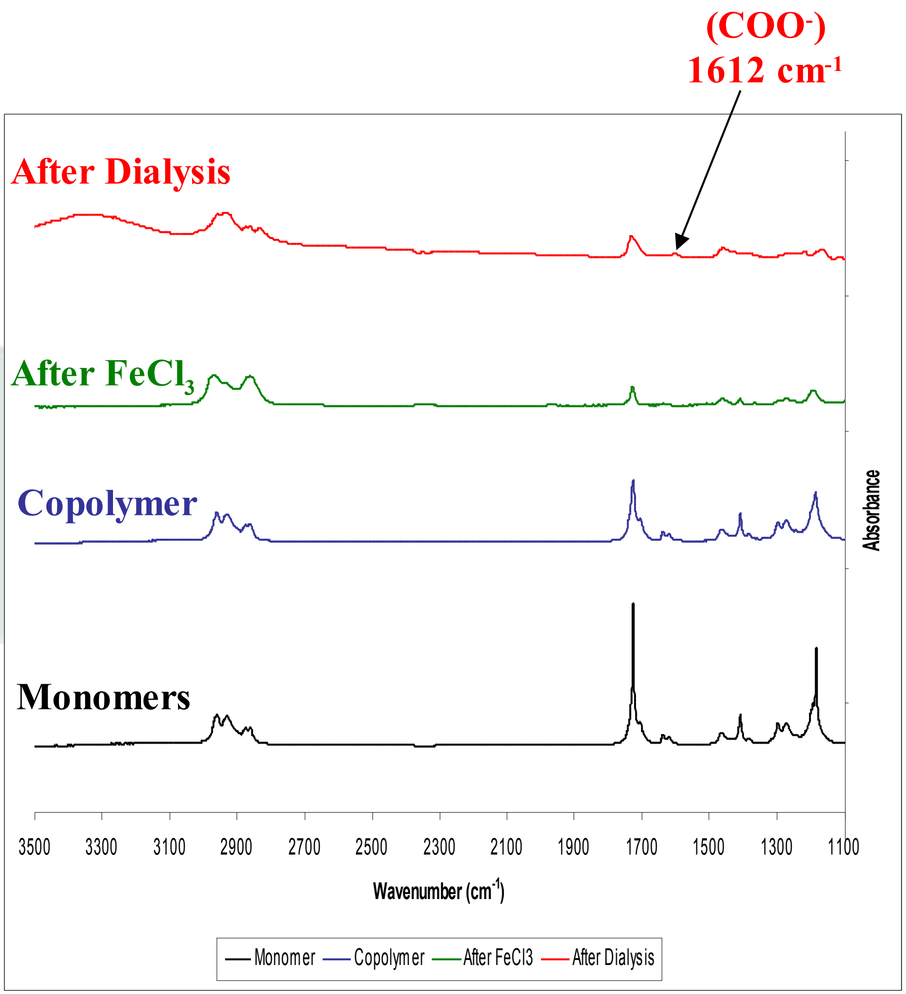

FTIR to confirm formation of the ionomer

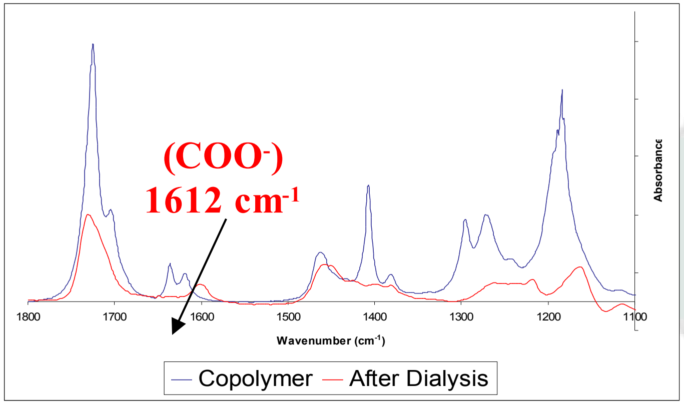

New peak appears at 1612 cm^{-1} after dialysis
- carboxylate salt stretching